

Article

# Calculation Model and Rapid Estimation Method for Coal Seam Gas Content

Fakai Wang <sup>1</sup>, Xusheng Zhao <sup>2</sup>, Yunpei Liang <sup>1,\*</sup>, Xuelong Li <sup>1,\*</sup>  and Yulong Chen <sup>3,\*</sup>

<sup>1</sup> State Key Laboratory of Coal Mine Disaster Dynamics and Control, College of Resources and Environmental Science, Chongqing University, Chongqing 400044, China; wangfakai316@126.com

<sup>2</sup> Chongqing Research Institute of China Coal Technology and Engineering Group Corp., Chongqing 400037, China; cq\_zxs@163.com

<sup>3</sup> State Key Laboratory of Hydrosience and Engineering, Tsinghua University, Beijing 100084, China

\* Correspondence: liangyunpei@126.com (Y.L.); lixlcumt@126.com (X.L.); chenyl@tsinghua.edu.cn (Y.C.)

Received: 27 September 2018; Accepted: 12 November 2018; Published: 14 November 2018



**Abstract:** Coalbed gas content is the most important parameter for forecasting and preventing the occurrence of coal and gas outburst. However, existing methods have difficulty obtaining the coalbed gas content accurately. In this study, a numerical calculation model for the rapid estimation of coal seam gas content was established based on the characteristic values of gas desorption at specific exposure times. Combined with technical verification, a new method which avoids the calculation of gas loss for the rapid estimation of gas content in the coal seam was investigated. Study results show that the balanced adsorption gas pressure and coal gas desorption characteristic coefficient ( $K_t$ ) satisfy the exponential equation, and the gas content and  $K_t$  are linear equations. The correlation coefficient of the fitting equation gradually decreases as the exposure time of the coal sample increases. Using the new method to measure and calculate the gas content of coal samples at two different working faces of the Lubanshan North mine (LBS), the deviation of the calculated coal sample gas content ranged from 0.32% to 8.84%, with an average of only 4.49%. Therefore, the new method meets the needs of field engineering technology.

**Keywords:** gas pressure; gas content; gas basic parameters; rapid estimation technology

## 1. Introduction

The basic parameters of coalbed gas are the foundation for preventing and controlling coal and gas outbursts [1]. As one of the most important basic parameters [2], coalbed gas content is employed to calculate the coal seam gas reserves, predicting gas emission from mines, and evaluating coal and gas outburst risk. Measuring coalbed gas content accurately is required to reduce the occurrence of mine disasters and the cost of mine gas hazard prevention [3]. At present, several methods have been proposed to determine the coalbed gas content, which can be roughly divided into direct and indirect methods. The indirect method is primarily used to calculate the gas content of coal through the Langmuir equation. However, this method has the disadvantages of in situ measurement process complexity and poor accuracy. Therefore, downhole direct measurement methods [4] have been widely used.

Many works have been conducted on theoretical and experimental studies of the estimation of gas content directly in the downhole. Jin and Firoozabadi [5] have studied phase behavior and flow in nanopores using density functional theory and various molecular simulations. Zhao et al. [1] present adsorption and desorption isotherms of methane, ethane, propane, n-butane, and isobutane, as well as carbon dioxide, for two shales and isolated kerogens determined by a gravimetric method. Bertard et al. [6] found that the early adsorption diffusion process of gas was proportional to the square

of the time and formed a direct measurement method of coal seam gas content. This method predicts the gas loss through the gas desorption data and derivation equation, thus laying the foundation for determining the gas loss in the sampling process. McCulloch et al. [7] simplified the Bertard method and proposed a United States Bureau of Mines (USBM) direct gas content estimation method that is the square root calculations of desorption time ( $\sqrt{t}$ ), and is proportional to the cumulative desorption. Ulery and Hyman [8] proposed a modified determination method (MDM) based on the measurement of various gas pressures, then the ideal gas law is used to calculate the desorption of gases under standard temperature and pressure conditions (STP). Mavor et al. [9,10] established a process for the estimation of gas content based on the USBM direct assay. Saghafi et al. [11] showed that the initial desorption of coal gas has an exponential relation with time. Smith and Williams [12] proposed a technique for the direct estimation of coal sample gas content from exposed rotary boreholes. Chase [13] determined the coal gas content by plotting the gas desorption rate curve and the cumulative desorption curve using the least squares method. Sawyer et al. [14] found that it is difficult to obtain more accurate gas desorption amounts and the residual gas volume by prematurely breaking the coal sample during desorption. Chen et al. [15] found that using an equation or method that does not have a large correlation with the gas desorption feature to calculate the gas content is usually more error-prone. Chen et al. [16] concluded that the negative exponential equation method is more consistent with the gas desorption law in the initial stage of tectonic coal. Lei et al. [17] proposed a new method of improvement based on the Barrer equation method to improve the accuracy of gas content measurement in coal seams. Zhang et al. [18] determined the gas desorption law of coal samples in different gas pressure conditions by experiments and proved that the  $\sqrt{t}$  method is more consistent with the gas desorption law in the initial stage. Li and Yang [19] calculated and compared the gas loss in the sampling process using the graphic method and least squares method. The “Direct Gas Content Measurement Device (DGC)” [20–27], which was developed based on an empirical equation, can determine the gas content of coal. The calculation of the gas content is based on the law of gas desorption. The empirical equations of gas desorption in coal, which have been proposed by scholars throughout the world, are listed in Table 1.

**Table 1.** Coal gas desorption equations.

Equations	$Q_t$ (mL/g)	Applicable Conditions
Barrer [28]	$\frac{Q_t}{Q_\infty} = \frac{2s}{V} \sqrt{\frac{D_t}{\pi}}$	$0 \leq \sqrt{t} \leq \frac{V}{2s} \sqrt{\frac{\pi}{D}}$
Winter [29]	$Q_t = \frac{v_1}{1-k_t} t^{1-k_t}$	$0 < k_t < 1$
Wang [30]	$Q_t = \frac{ABt}{1+Bt}$	
Sun [31]	$Q_t = at^i$	$0 < i < 1$
Exponential [32]	$Q_t = \frac{v_0}{b} (1 - e^{-bt})$	

Barrer [28] concluded that adsorption-desorption is a reversible process, and the cumulative amount of gas absorbed or desorbed is proportional to the square root of time. Winter et al. [29] found that the change in the amount of desorbed gas over time can be expressed as a power equation. Wang et al. [30] believed that the gas desorption of coal with time is consistent with the Langmuir adsorption equation. Sun [31] confirmed that gas desorption in coal is mainly a diffusion process, and the change of desorption gas content with time can be expressed by a power equation. Others [32] believe that the decay process of coal gas desorption with time conforms to the exponential equation. Due to the extensive variety of research objects, the empirical equation has both reasonable and unreasonable components in revealing the law of gas desorption in coal [33]. Compared with the equations in Table 1, calculating the gas compensation amount is difficult due to three shortcomings. First, the definition of the gas desorption start time (zero time, as shown in Figure 1) is ambiguous. Second, the percentage of lost gas and original gas in the coal sample varies with different degrees of metamorphism and damage types. The model that is established by the derivation equation and the

basic theory of the model have different assumptions, and the existence of these hypotheses may be very contradictory to the real environment. Therefore, the best method for measuring the gas content is to avoid the calculation of the gas loss.

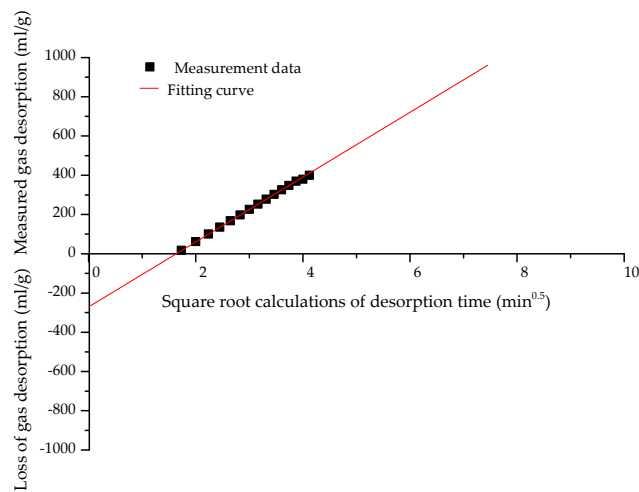


**Figure 1.** Diagram of gas desorption loss estimation.

In this paper, an analysis of the simulation results in gas desorption was performed, and a combination of numerical analysis and field tests were conducted. In order to improve the coalbed gas content measuring accuracy, a rapid method for determining the gas content in coal seams to avoid the calculation of gas loss was proposed for on-site measurement of the gas content in coal seams, which can accurately provide the basic parameters for mine safety production.

## 2. Experimental Study

### 2.1. Experimental Apparatus

To simulate the gas desorption process of a coal sample, a set of simulation equipment was designed and developed. A schematic of the experimental setup is shown in Figure 2.

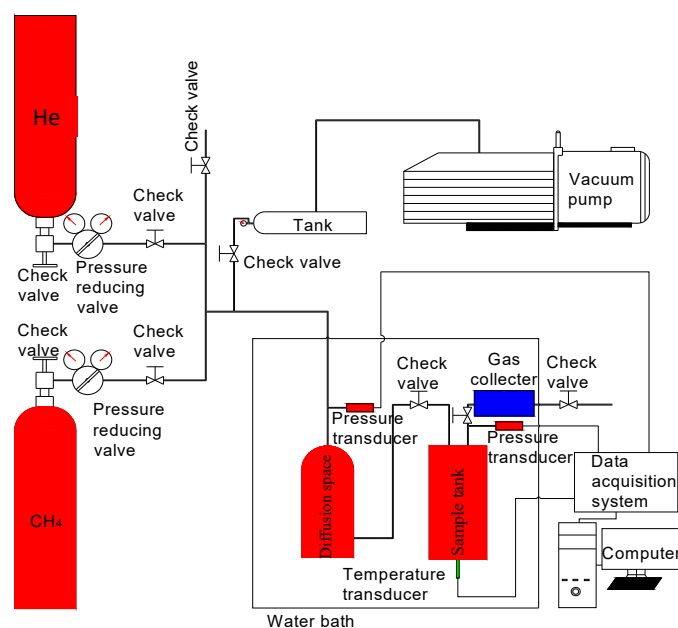


**Figure 2.** Schematic of the experimental setup.

The experimental device consisted of four systems, the details of each system are listed as follows:

- (1) Vacuum system: This system consisted of a composite vacuum gauge, a vacuum pump, a vacuum tube, a vacuum gauge, and a glass three-way valve.
- (2) Constant temperature system: This system consisted of a constant temperature water bath, a coal sample tank, a diffusion tank, a precision pressure gauge, and a high-purity methane gas source.
- (3) Adsorption balance system: This system consisted of precision pressure gauges, methane gas sources, inflatable tanks, coal sample tanks, and valves.
- (4) Desorption measurement control system: This system consisted of a pressure control valve and a homemade gas desorption analyzer.

To eliminate the influence of temperature on the simulation results, the device could achieve a constant ambient temperature in the coal sample gas adsorption-desorption process.

## 2.2. Coal Sample Preparation

The coal sample was taken from the No. 3 coal seam in the Lubanshan North Mine (LBS), which is located in Yibin City of Sichuan Province, and primarily consisted of lean coal. The location of the mine is shown in Figure 3. The No. 3 coal seam of LBS is located in the lower part of the Shanxi Formation, with an average distance of 58.04 m from No. 9 and an average thickness of 6.71 m. Figure 4 shows a general sketch of the coal seams and a diagram of the coal seam gas pressure measurement. The roof of the coal seam is mudstone and sandy mudstone, and the bottom slab is sandy mudstone and dark gray sandstone.



**Figure 3.** Geographical location of the LBS.

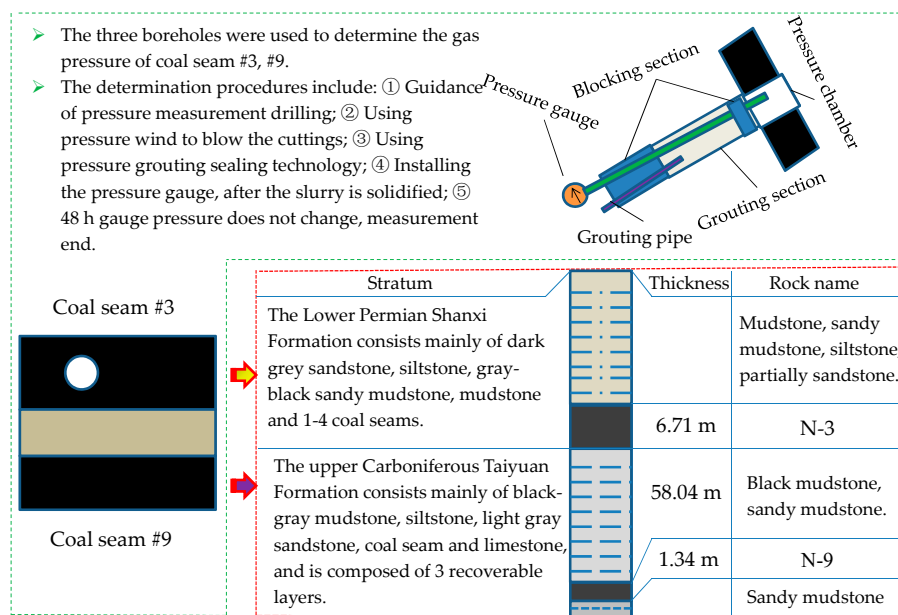


**Figure 4.** General sketch of the coal seam and a diagram of coal seam gas pressure measurement.

Coal seam No. 3 was sampled and marked as N-3. According to the “Sampling of coal seams” [34], coal samples were taken from the same coal seam at the same location. Five samples of coal with different damage types were collected, each with a mass of 5 kg, and were sealed and sent to a laboratory for the preparation of experimental coal samples. According to the experimental requirements, the parameters, such as the hardness coefficient, true relative density, and proximate analysis of the coal, need to be separately determined. Therefore, the coal sample collected at the site must be processed into a sample that satisfies these requirements. In addition, the gas pressure (1.2 MPa) and coal seam temperature (35 °C) in the N-3 coal seam were measured on site, as shown in Figure 4.

According to “Methods for determining coal hardness coefficient” [35], a sample for the estimation of the coal hardness coefficient was prepared as follows: A coal sample of 1000 g was crushed and screened using standard sieves with apertures of 20 mm and 30 mm. Next, 50 g of the prepared sample was weighed into 1 part, with one set for every 5 parts, and a total of 3 groups were weighed. The coal hardness coefficient to be measured was applied.

According to “Proximate analysis of coal” [36], samples for proximate analysis and estimation were prepared as follows: 500 g of raw coal was crushed and sieved to create samples of coal with a size less than 0.2 mm, and placed in a ground jar for sealing. Three samples were prepared; each sample’s weight exceeded 50 g.

According to “Methods for determining the block density of coal and rock” [37], samples for density analysis and determination were prepared as follows: 50 g of raw coal was crushed and sieved to create samples of granular coal with a size less than 0.2 mm, and kept in a grinding jar sealed for use. Three samples were prepared; each sample’s weight exceeded 2 g. Figure 5 shows the coal sample processing flow and related test equipment.

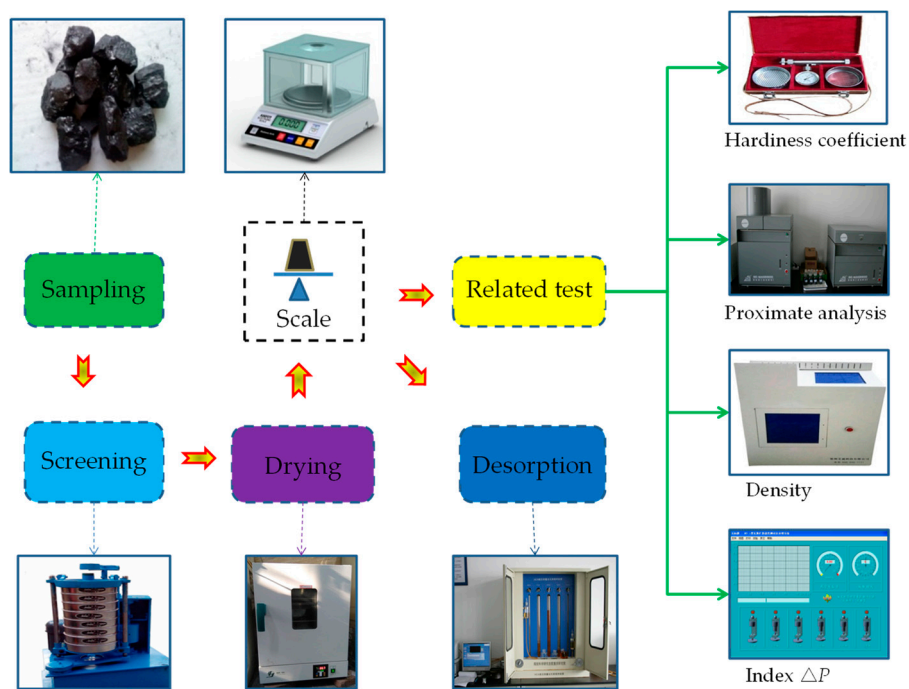


Figure 5. Coal sample preparation processes.

The preparation process of the desorption coal sample is described as follows: The raw coal was crushed and sieved to create 200 g of granules with sizes that ranged between 1 mm to 3 mm sieves. All samples were placed in a dryer at 105 °C for 3 h. After cooling, the coal samples were placed in a container isolated from air and sealed for subsequent use. Details of the coal samples are listed in Table 2.

Table 2. Preparation of coal samples with different specifications.

Term	Particle Size (mm)	Quality (g)	Quantity (parts)
Hardiness coefficient	20~30	50	15
Proximate analysis	<0.2	50	3
Density	<0.2	2	3
Adsorption constant	0.2~0.25	50	1
Desorption property	1~3	200	1

The preparation of coal samples with different specifications was used to determine relevant parameters and the coal sample gas desorption characteristic coefficient ( $K_t$ ). Based on these indicators, the coal seam outburst risk assessment and coal seam classification could be carried out, and the index  $K_t$  could be calculated.

### 2.3. Experimental Procedure

The coal sample gas desorption process simulation was conducted by employing the experimental device shown in Figure 2. Since the gas desorption environment of the sample was always maintained at a temperature of  $30 \pm 1$  °C and a gas outlet pressure of 0.1 MPa during the measurement process, the gas desorption of the sample could be considered to be an isothermal and isostatic desorption process. Dried coal samples with a weight and particle size ranging from 60 g to 80 g and 1 mm to 3 mm, respectively, were firstly loaded into the coal sample tank. After loading the coal sample, the sample tank was sealed and vacuumed with a water bath temperature of 35 °C until the pressure was less than 20 Pa. Then, methane with a purity of 99.9% was inlet into the diffusion tank with a defined pressure. After that, the sample tank and diffusion tank were connected to permit methane gas flow into the sample tank and begin the adsorption process. The adsorption process was considered

finished only when the pressure in both the diffusion and sample tanks stayed constant, and this process usually continued for nearly 48 h. The gas desorption process began after the system pressure remained constant. The amount of desorption gas should be recorded every 30 s, and the test should be stopped after desorption for 30 min. The gas desorption capacity needs to be converted to the standard condition volume, and the conversion equation [38] is as follows:

$$W_t = \frac{273.2}{101325(273.2 + t_w)} (P_{\text{atm}} - 9.81h_w - P_S) \cdot W_t' \quad (1)$$

where  $W_t$  is the total amount of gas desorption in the standard state (mL),  $W_t'$  is the total gas desorption measured in the experimental environment (mL),  $t_w$  is the water temperature in the tube ( $^{\circ}\text{C}$ ),  $P_{\text{atm}}$  is atmospheric pressure (Pa),  $h_w$  is the height of the water column in the measuring tube (mm), and  $P_S$  is the saturated water vapor pressure (Pa).

### 3. Experimental Results

#### 3.1. Related Parameter

Proximate analysis is the main indicator for understanding the characteristics and the basic basis for evaluating the metamorphism of coal [36]. Elemental analysis is an important indicator for studying the degree of metamorphism of coal and estimating its carbonized product. It is also the basis for calorific calculation for coal as a fuel in industry. The proximate analysis indexes and elemental analysis indexes of the coal samples are listed in Table 3.

**Table 3.** Result of proximate analysis indexes and elemental analysis indexes.

Proximate Analysis Indexes						Elemental Analysis Indexes			
$M_{\text{ad}}$ (%)	$A_{\text{ad}}$ (%)	$V_{\text{daf}}$ (%)	$S_{\text{t,d}}$ (%)	$C_{\text{daf}}$ (%)	$Q_{\text{b,d}}$ (MJ/kg)	$G_{\text{R,I}}$	$H_{\text{daf}}$ (%)	$O_{\text{daf}}$ (%)	$N_{\text{daf}}$ (%)
1.15	17.67	16.12	0.31	65.06	29.41	11.2	4.30	2.53	1.50

Notes:  $M_{\text{ad}}$  is the air dry basis moisture (%).  $A_{\text{ad}}$  is the air dry basis ash (%).  $V_{\text{daf}}$  is the dry ash-free basis of volatile content (%).  $S_{\text{t,d}}$  is the true relative density ( $\text{g}/\text{cm}^3$ ).  $Q_{\text{b,d}}$  is the calorific value (MJ/kg).  $G_{\text{R,I}}$  is the clean coal bond index (dimensionless).  $C_{\text{daf}}$  is the fixed carbon content (%).  $H_{\text{daf}}$  is the dry ash-free basis hydrogen content (%).  $O_{\text{daf}}$  is the dry ash-free basis oxygen content (%).  $N_{\text{daf}}$  is the dry ash-free basis nitrogen content (%).

In practice, the outstanding predictive index is an important indicator for the identification of outburst-prone coal seams [39]. The characteristic indicator and the adsorption constants are key indicators for quantifying the adsorption-desorption characteristic of coal. Table 4 lists the measured data of the relevant outstanding indicators of N-3 coal, the characteristic indexes, and the coal gas adsorption constants.

**Table 4.** Relevant indicator measured data.

Outstanding Predictive Indicators				Characteristics Indicators			Adsorption Constants	
$f$	$\Delta P$ (mmHg)	$D_{\text{cf}}$	$P$ (MPa)	$TRD$ ( $\text{g}/\text{cm}^3$ )	$ARD$ ( $\text{g}/\text{cm}^3$ )	$n$ (%)	$a_{\text{ac}}$ ( $\text{cm}^3/\text{g}$ )	$b_{\text{ac}}$ ( $\text{MPa}^{-1}$ )
0.395	29.1	IV	1.20	1.32	1.23	6.8	29.6786	1.3236

Notes:  $f$  is the coal hardness coefficient (dimensionless).  $\Delta P$  is the initial velocity of diffusion of coal gas (mmHg).  $D_{\text{cf}}$  is the degree of coal fracturing (dimensionless), as shown in Table 5.  $P$  is the measured coal seam gas pressure (MPa).  $TRD$  is the true relative density of the coal sample ( $\text{g}/\text{cm}^3$ ).  $ARD$  is the apparent relative density of the coal sample ( $\text{g}/\text{cm}^3$ ).  $n$  is the ratio of the total volume of tiny voids to the total volume of coal (%).  $a_{\text{ac}}$  and  $b_{\text{ac}}$  are Langmuir adsorption constants;  $a_{\text{ac}}$  is the maximum gas adsorption capacity ( $\text{cm}^3/\text{g}$ ) and  $b_{\text{ac}}$  is the adsorption constant ( $\text{MPa}^{-1}$ ).

**Table 5.** Classification of the degree of coal fracturing.

Class	I	II	III	IV	V
Degree of coal fracturing	Massive coal	Slightly fractured coal	Severely fractured coal	Pulverized coal	Completely pulverized coal

The coal hardness coefficient ( $f$ ) reflects the ability of coal to resist damage, and can be employed to predict the ability to resist breakage and its stability after drilling. When the index ( $f$ ) exceeds 0.5, the coal has a strong ability to resist outburst. A comparison of Tables 4–6 reveals that  $f$  is  $0.395 < 0.5$ , which indicates that coal N-3 is relatively easily destroyed under the gas pressure of 0.74 MPa.

**Table 6.** Thresholds of four indicators for the identification of outburst-prone coal seams.

Term	$D_{cf}$	$\Delta P$ (mmHg)	$f$	$P$ (MPa)
Thresholds	III, IV, V	$\geq 10$	$\leq 0.5$	$\geq 0.74$

The index ( $\Delta P$ ) of the initial velocity of the diffusion of coal gas is also one of the indicators for predicting the risk of coal and gas outburst [22,39], which can reflect the degree of gas emission from gas-filled coal bodies.  $\Delta P$  is 29.1 mmHg  $> 10$  mmHg, which indicates that the coal seam has a rapid dispersion and a strong destruction capability.

Porosity ( $n$ ) refers to the ratio of the mass of a certain substance contained in a certain volume to the mass and volume of the same substance at a specified temperature. The porosity of coal is not only an important index for measuring the development status of pores and cracks in coal, but also an important factor that affects the adsorption and infiltration capacity of coal.

The adsorption constants  $a_{ac}$  and  $b_{ac}$  were measured using a high-pressure volumetric method to determine the coalbed methane adsorption constants  $a_{ac}$  and  $b_{ac}$ . The adsorption constants  $a_{ac}$  and  $b_{ac}$  are calculated from the Langmuir adsorption equation [32,33] as follows:

$$Q = \frac{a_{ac}b_{ac}P}{1 + b_{ac}P} \quad (2)$$

where  $Q$  is the adsorption gas quantity (mL/g),  $P$  is the adsorption equilibrium gas pressure (MPa), and  $a_{ac}$  and  $b_{ac}$  are the Langmuir adsorption constants.

$a_{ac}$  and  $b_{ac}$  are determined by the amount of coal gas sample adsorbed under different pressures. Therefore, the gas adsorption constant of the coal is an indicator of coal gas adsorption capacity. The physical meaning of  $a_{ac}$  is the maximum gas adsorption capacity of coal.

### 3.2. Gas Desorption Process

The gas adsorption capacity of the coal samples was calculated based on the gas adsorption equilibrium pressures and the results for the related parameters, by using the Langmuir adsorption equation. The simulation results are shown in Figure 6.

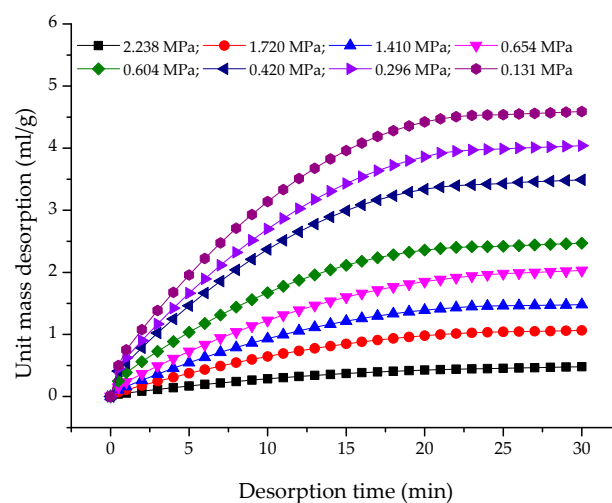


**Figure 6.** Desorption curves under different adsorption equilibrium gas pressures.

As shown in Figure 6, with an increase in the gas pressure, the coal samples with a unit mass are located at the same time point. The amount of desorption gas also gradually increases, but its increase decelerates, which mainly resulted from the primary limitation of the internal pores of the coal body. In addition, the slope of the gas desorption curve decreases and gradually flattens as the exposure times of the coal samples increase, which can be attributed to the decrease of adsorption gas and the complexity of the pore structure of coal [14,16]. During the initial stage of exposure, the gas concentration in the large pores of the coal body was released outward, and the resistance to gas migration was large; whereas in the later stage, the primary factor for determining the gas release rate was the large number of pores and fractures in the coal. The diffusion coefficient of gas will be reduced by one to two orders of magnitude.

Figure 7 shows the relationship between the gas desorption amount and the time for different gas pressures.

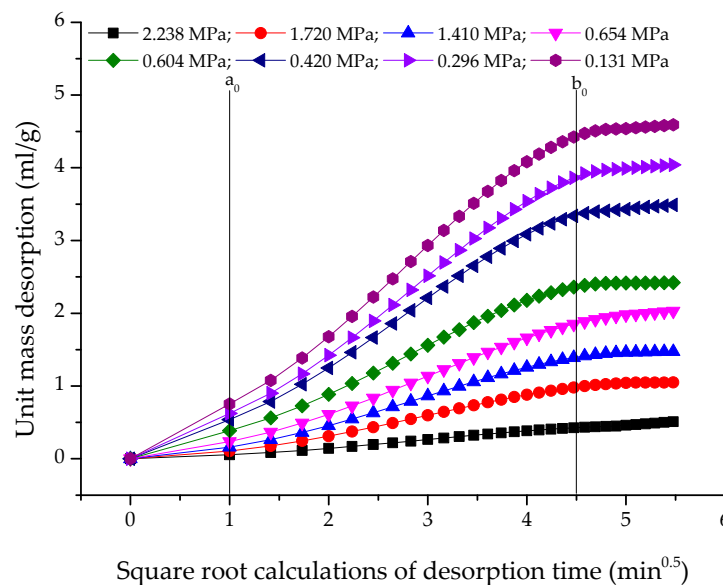


**Figure 7.** Relationship between the gas desorption amount and the square root of desorption time.

As shown in Figure 7, the gas desorption amount and the square root of the gas desorption time are linear. However, with the extension of the exposure time of the coal sample, the slope of the straight line will slightly decrease. The square root of the distinct turning point at the gas desorption time is  $1 \text{ min}^{0.5}$  and  $4.5 \text{ min}^{0.5}$ ; since the start of desorption, the slope of the line gradually increased and then decreased. The square root of the gas desorption time exceeds  $4.5 \text{ min}^{0.5}$ . The slope of the straight line is less than the slope of the straight line at the initial stage and gradually decreases; the square root of the gas desorption time falls between  $1 \text{ min}^{0.5}$  and  $4.5 \text{ min}^{0.5}$ . As the gas pressure in the coal seam increases, the slope of the straight line increases. According to the calculation model of Winter [29], the change in the gas desorption rate with time can be expressed by an exponential equation [31] for certain other conditions as follows:

$$V_t = V_a \left( \frac{t}{t_a} \right)^{K_t} \quad (3)$$

Then, Equation (4) can be derived as follows:

$$K_t = \frac{\ln V_a - \ln V_t}{\ln t - \ln t_a} \quad (4)$$

Here,  $K_t$  is the gas desorption characteristic coefficient whose exposure time ranges from 1 min to 5 min ( $\text{mL}/(\text{g} \cdot \text{min}^{0.5})$ ).  $V_t$  and  $V_a$  are the gas desorption speed of coal samples with unit mass at the time  $t$  and  $t_a$ , respectively ( $\text{cm}^3/\text{min}$ ).  $t$  and  $t_a$  are the gas desorption time and time in min, respectively.

The results were converted to the amount of gas desorbed from the coal sample, and the index ( $K_t$ ) was determined by the least squares method. The results are listed in Table 7.

**Table 7.** Gas adsorption capacity and gas desorption characteristic coefficient ( $K_t$ ).

$P$ (MPa)	$Q$ (mL/g)	$K_1$ (mL/(g·min <sup>0.5</sup> ))	$K_2$ (mL/(g·min <sup>0.5</sup> ))	$K_3$ (mL/(g·min <sup>0.5</sup> ))	$K_5$ (mL/(g·min <sup>0.5</sup> ))
0.131	4.72	0.1467	0.1380	0.1268	0.1202
0.296	6.92	0.2895	0.2644	0.2582	0.2292
0.420	8.20	0.3660	0.3568	0.3533	0.3274
0.604	9.70	0.4891	0.4434	0.4059	0.3852
0.653	10.04	0.5405	0.5067	0.4764	0.4326
1.410	13.40	0.7702	0.7176	0.6783	0.6283
1.720	14.20	0.8428	0.7897	0.7148	0.6470
2.238	15.19	0.9395	0.8846	0.8555	0.7991

Notes:  $P$  is the gas pressure (MPa).  $Q$  is the adsorption gas quantity (mL/g).  $K_t$  is the gas desorption characteristic coefficient whose exposure time ranges from 1 min to 5 min (mL/(g·min<sup>0.5</sup>)).

As shown in Table 7, under the same adsorption-balanced gas pressure, different desorption characteristic coefficient values gradually decrease from  $K_1$  to  $K_5$  with the exposure time of the experimental coal sample; that is,  $K_1 > K_2 > K_3 > K_4 > K_5$ . First, this result is attributed to the gradual decrease of adsorbed gas and the decrease of the amount of available desorption gas. Second, with the accumulation of the amount of desorption gas in fixed space, the gas pressure in the fixed space and the pressure gradient in the coal gas gradually decrease. For the same gas desorption characteristic coefficient,  $K_t$  gradually increases with an increase in the adsorption equilibrium gas pressure. The larger the adsorption equilibrium gas pressure, the larger the amount of gas adsorbed by the coal sample under the larger adsorbed gas pressure gradient. When the gas is desorbed into the fixed space, the larger the gas pressure gradient between the fixed space and the coal sample, the larger the amount of gas desorption per unit time.

As the exposure time increases, the gas pressure gradients between adsorbed-balance gas and fixed-space cumulative gas gradually decrease, and the amount of desorption gas will gradually decrease during the unit exposure time. Therefore,  $K_t$  can be considered to be a reflection of the physical quantity of the gas desorption speed at different times.

## 4. Discussion

### 4.1. Relationship between Gas Pressure and $K_t$

The relationships between gas pressure and gas desorption characteristic coefficients are shown in Figure 8.

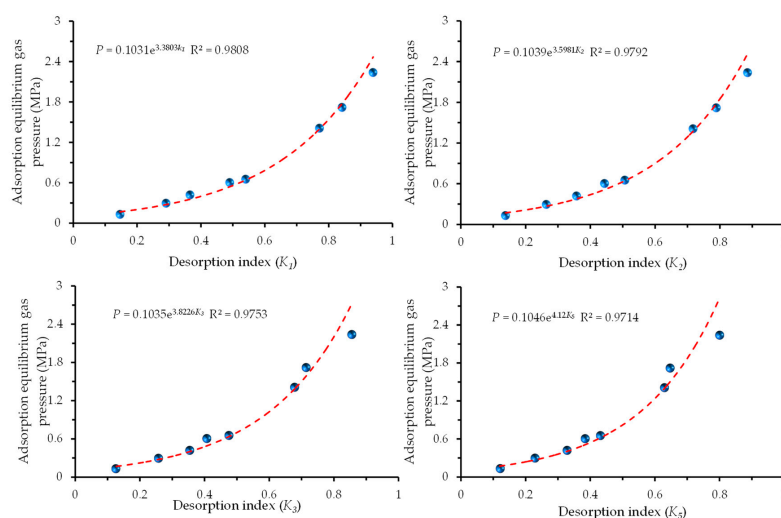


**Figure 8.** Relationships between gas pressure and gas desorption characteristic coefficients.

As shown in Figure 8, the gas desorption characteristic coefficient ( $K_t$ ) also increases, and the increase in amplitude is gradually increased with gas pressure. Because coal is a natural adsorbent, the larger the adsorption pressure, the larger the amount of gas adsorption and the larger the amount of gas that is desorbed [31]. For the same gas desorption characteristic coefficient, the index ( $K_t$ ) gradually increases with an increase in the adsorption equilibrium gas pressure. According to the adsorption theory of Langmuir [33], under the action of the larger adsorption equilibrium gas pressure, the coal sample absorbs a larger amount of gas. When the gas is desorbed into the fixed space, a larger pressure gradient of desorption gas is generated between the fixed space and the coal sample to promote coal adsorption equilibrium gas desorption.

For the coal seam adsorption equilibrium gas pressure and the different  $K_t$  respectively, trend fitting is available. The adsorption equilibrium gas pressure and the different  $K_t$  are exponential equation relations and have good correlation, the coefficient of determination ( $R^2$ ) being higher than 0.97.

A comparison of the correlation curve of the gas pressure and  $K_t$  at different exposure times is shown in Figure 8. The results indicate that  $R^2$  decreases to a minor extent with the exposure time of the coal sample due to the deviation of the gas desorption amount error caused by the increase in the exposure time [16,40]. However, the  $R^2$  of the coal sample gas desorption regression fitting curve remains greater than 0.97, the correlation of regression fitting curve is higher, and the result is reliable. Therefore, the gas pressure can be expressed as follows:

$$P = A_c e^{B_c K_t} \quad (5)$$

where  $A_c$  and  $B_c$  are the constants that correspond to different desorption times, which are dimensionless;  $P$  is the adsorption equilibrium gas pressure (MPa); and  $K_t$  is the gas desorption characteristic coefficient that corresponds to different desorption times ( $\text{mL}/(\text{g}\cdot\text{min}^{0.5})$ ).

#### 4.2. Relationship between Gas Content and $K_t$

The relationships between gas content and gas desorption characteristic coefficients are shown in Figure 9.

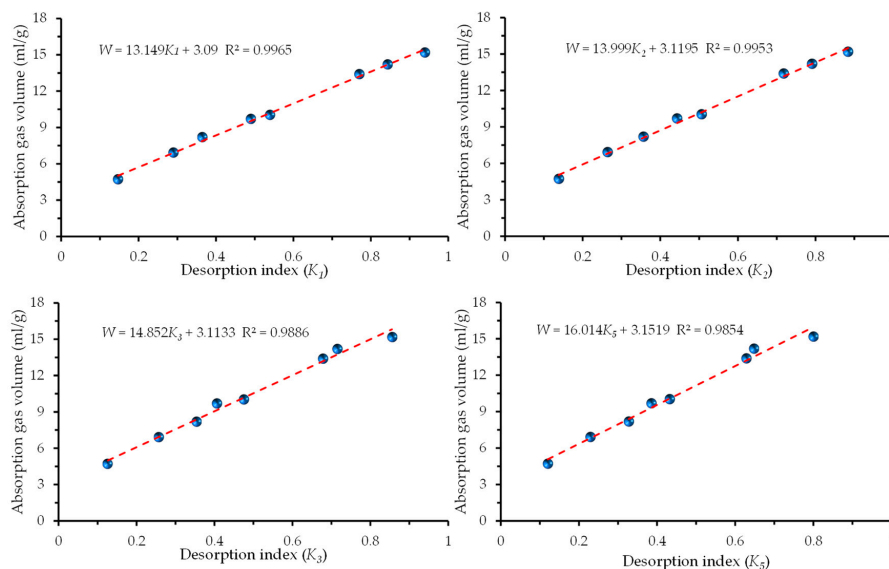


**Figure 9.** Relationships between gas content and gas desorption characteristic coefficients.

As shown in Figure 9, the gas content increases as  $K_t$  increases. Coal is a natural adsorbent with double pores and fissures. The larger the gas content, the larger  $K_t$  is. According to the adsorption theory equation of Langmuir [32], the larger the gas content, the larger the gas pressure, and the larger the amount of adsorbed coal gas. The larger the amount of adsorption gas in the coal sample, the larger the index  $K_t$ .

The coal seam gas content and  $K_t$  have a linear equation relationship and an excellent correlation. The correlation coefficient of the regression fitting curve showed a slight decrease with the exposure time. With an increase in desorption time, the deviation of the desorption amount of the coal sample gas gradually increases. However,  $R^2$  remains greater than 0.98, which means the regression fitting curve has higher correlation and the result is reliable. Therefore, the relationship between the gas content and  $K_t$  can be expressed by Equation (6) as follows:

$$W = \partial K_t + \beta \quad (6)$$

where  $\partial$  and  $\beta$  are the constants that correspond to different desorption times (dimensionless),  $W$  is the gas adsorption amount (mL/g), and  $K_t$  is the gas desorption characteristic coefficients that correspond to different desorption times (mL/(g·min<sup>0.5</sup>)).

According to the adsorption theory equation of Langmuir [32], the gas pressure and gas content are not linear. To analyze the accuracy of the relationship between the coal seam gas pressure, and gas content and  $K_t$  for different exposure times,  $R^2$  at different times is compared and listed in Table 8.

**Table 8.** Comparison of the coefficient of determination ( $R^2$ ) under different exposure times.

Term	$P = A_c e^{B_c K_t}$	$W = \partial K_t + \beta$	Exposure Time (min)
$R^2$	0.98079	0.99653	1
	0.97922	0.99531	2
	0.97535	0.98858	3
	0.97140	0.98542	5
average of $R^2$	0.97669	0.99146	

As shown in Table 8, for  $R^2$ , the  $K_t$  used to describe the coal sample gas content and gas pressure at different exposure times can reach a high accuracy, especially when  $K_t$  is used to describe the gas content. The maximum  $R^2$  is 0.99146.

Although, with the extension of exposure time, the  $K_t$  to describe coal gas pressure and gas content has a certain decrease; the decrease range is very small within 5 min, and the effect on the accuracy of the results is negligible.

### 4.3. Technical Verification

#### 4.3.1. Experimental Verification

Based on the experimental data, the method proposed in this paper was used to calculate and revise the gas content of the coal samples under two different pressures after exposure for 1 min, 2 min, 3 min, and 5 min. The calculation results of the gas content and the calculation deviation are listed in Table 9.

**Table 9.** Calculated values and deviation of gas content.

Gas Pressure (MPa)	Gas Content (mL/g)	Exposure Time (min)	$K_t$ (mL/(g·min <sup>0.5</sup> ))	Calculated Gas Content (mL/g)	Deviation (%)
0.64	9.95	1	0.4634	9.18	−7.73
		2	0.4232	9.04	−9.14
		3	0.4114	9.22	−7.33
		5	0.3860	9.33	−6.23
0.912	11.51	1	0.6309	11.39	−1.04
		2	0.5351	10.61	−7.81
		3	0.5137	10.74	−6.68
		5	0.5262	11.58	0.60

According to Table 9, the gas content calculated deviation range was from −9.14% to 0.6%, with an average of only 3.23%, which indicates that the new method can accurately calculate the gas content of coal samples. In addition, for the conditions of different adsorption equilibrium gas pressures,

the calculated and measured gas content values are the smallest when the coal sample is exposed for 5 min, which indicates that the longer the exposure time, the closer the calculated gas content is to the measured value.

#### 4.3.2. Field Verification

To test the reliability of the new method, the gas content of the N-3 coal seam in the LBS was measured.

The test sites were the E2305 inlet and the northern inlet of the LBS. The downhole gas desorption apparatus was used to directly measure the downhole desorption section of the coal sample. The underground gas desorption operation flow chart is shown in Figure 10. A total of six groups were tested, of which E2305 entered the air in 5 samples and the north inlet entered the air in 1 sample. The gas content measurement and calculation results are listed in Table 10.

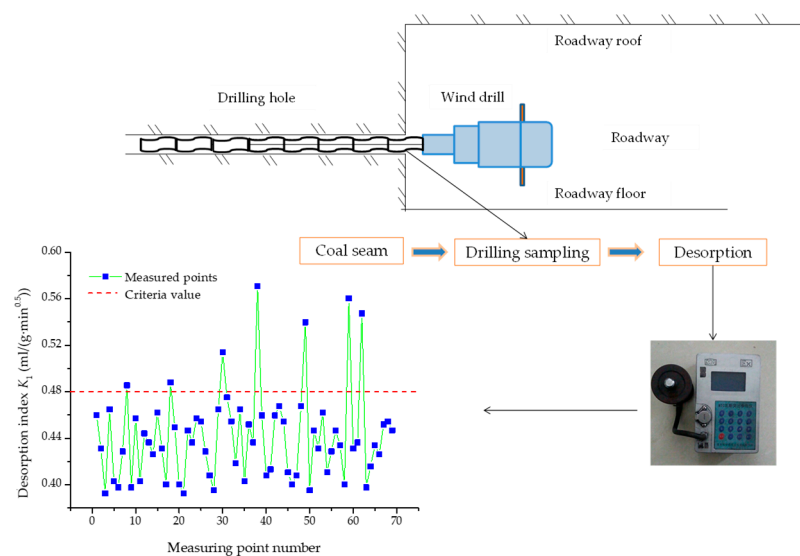


Figure 10. On-site gas desorption flow chart.

Table 10. Comparison of measured and calculated values of gas content.

Number	$K_5$ (mL/(g·min <sup>0.5</sup> ))	Calculated Values (mL/g)	Measured Values (mL/g)	Deviation (%)
1	0.4153	9.80	10.10	−2.97
2	0.3925	9.43	9.40	0.32
3	0.3611	8.93	9.41	−5.1
4	0.4385	10.17	10.71	−5.0
5	0.5186	11.45	10.93	4.76
6	0.40225	9.59	10.52	−8.84

Note: coal sample exposure time is 5 min.

As shown in Table 10, using the new method to measure and calculate the gas content of the coal seam at two different working faces of the LBS, the deviation of the calculated gas content ranged from 0.32% to 8.84%, with an average of only 4.49%. The main reasons for this finding are as follows: The coal sample is impure when it is collected by the method of powdered coal through holes due to coal expansion. Therefore, as the exposure time of the shallow coal bodies increases and the desorption rate of gas decreases, the  $K_5$  calculated from the desorption law is also smaller than the actual  $K_5$ , which directly causes the calculated gas content of the new method to be smaller than the real gas content. When the indirect method is used to determine the gas content, the desorption rate that is measured at the site is less than the real desorption rate and will only affect the calculation of the loss and a part of the desorption amount, and the influence on the gas content of the raw coal is small.

Temperature has a significant effect on the gas adsorption and desorption of coal. The isothermal adsorption-desorption experiment is performed in the condition of the coal seam temperature, which is easily controlled. In field applications, there is a temperature difference between the coal seam and the roadway due to the cooling effect of the roadway; that is, the temperature of the coal sample changed when it was removed from the coal seam. This weak temperature change will have a certain influence on the coal gas content measurement results. From the point of view of field applications, the temperature difference between the coal seam and the roadway has a minimal effect on the final result of the new method.

The difference between the measured value and the calculated value using the new method of the gas content of coal sample exposure within 5 min is not distinct. The results conclude that the new method can accurately estimate the gas content of the coal seam in a field application, and the accuracy satisfies engineering needs. Therefore, the “calculation model and rapid estimation method of coal seam gas content” can be implemented in the field.

## 5. Conclusions

This paper is based on the analysis of simulation results in gas desorption and applies a field application for the investigation. A set of independently developed experimental apparatus was used to measure the gas desorption process of coal with a particle size of 1–3 mm in the N-3 coal seam of the LBS to research the relationship between the gas desorption law and the gas content. According to the specific exposure time of the gas desorption, the eigenvalues of the rules, and the establishment of a method for the rapid estimation of gas content in coal seams, the following main conclusions are obtained:

- (1) The gas desorption amount and the square root of the gas desorption time are linear, and the slope of the straight line will slightly decrease with the extension of the exposure time. The slope of the straight line is less than the slope of the straight line at the initial stage and gradually decreases; the square root of the gas desorption time falls between  $1 \text{ min}^{0.5}$  and  $4.5 \text{ min}^{0.5}$ . As the gas pressure increases, the slope of the straight line increases.
- (2) Simulation and verification of the on-site gas desorption law verified that the gas pressure and gas content of coal seams and  $K_t$  have an exponential equation and a linear equation relationship, respectively. Using this equation relationship, a new method for accurately calculating the gas content of underground coal seams is constructed.
- (3) Simulation experiments determined that the exposure time of the coal sample should be controlled within 5 min when using the new method to calculate gas content in a coal seam. The calculation equations at 1 min, 2 min, 3 min, and 5 min were given. The method can be used to calculate the coal seam gas content, and the deviation is within the allowable range of the project. Thus, this method can satisfy the needs of rapid gas content estimation at the site.

In this paper, the method for the calculation model and the rapid estimation of the gas content is simple and concise with respect to the operation and measuring accuracy. Changes in the ambient temperature of the test site will have an impact on the accuracy of the final result during field application, but this effect is negligible.

**Author Contributions:** Conceptualization, Y.L.; Methodology, X.Z.; Validation, F.W.; Formal Analysis, X.L.; Data Curation, Y.C.; Writing-Original Draft Preparation, F.W.; Writing-Review and Editing, X.L.; Funding Acquisition, Y.L.

**Funding:** This research received no external funding.

**Acknowledgments:** This study is financially supported by the National Science and Technology Major Project of China (Grant No. 2016ZX05043005), the State Key Research Development Program of China (Grant No. 2016YFC0801404 and 2016YFC0801402), and the National Natural Science Foundation of China (51674050), which are gratefully acknowledged. The authors also thank the editor and anonymous reviewers for their valuable advice.

**Conflicts of Interest:** The authors declare no conflict of interest.

## Nomenclature

$Q_t$	cumulative amount of desorbed gas from time $t = 0$ to time $t$ , mL/g
$Q_\infty$	ultimate adsorption-desorption gas amount, mL/g
$S$	unit mass sample outer surface area, $\text{cm}^2/\text{g}$
$V$	unit mass volume of coal sample, mL/g
$D$	diffusion coefficient, $\text{cm}^2/\text{min}$
$v_1$	gas desorption speed at $t = 1$ min, $\text{mL}/(\text{g}\cdot\text{min})$
$k_1$	characteristic coefficient of gas desorption speed change
$v_0$	gas desorption speed at $t = 0$ min, $\text{mL}/(\text{g}\cdot\text{min})$
$A$	cumulative gas desorption amount from start to time $t$ , mL/g
$B$	desorption constant, dimensionless
$a, i$	constants related to the gas content and structure of coal, dimensionless
$b$	gas desorption speed decay coefficient with time, dimensionless
$W_t$	total amount of gas desorption in the standard state, mL/g
$W_t'$	total gas desorption measured in the experimental environment, mL/g
$t_w$	water temperature in the tube, $^\circ\text{C}$
$P_{\text{atm}}$	atmospheric pressure, MPa
$h_w$	height of the water column in the measuring tube, mm
$P_S$	saturated water vapor pressure, MPa
$V_t, V_a$	gas desorption speeds of the coal samples with unit mass at time $t$ and $t_a$
$t, t_a$	gas desorption time and time in min
$K_t$	gas desorption characteristic coefficient whose exposure time ranges from 1 min to 5 min
$M_{\text{ad}}$	air dry basis moisture, %
$A_{\text{ad}}$	air dry basis ash, %
$V_{\text{daf}}$	dry ash-free basis of volatile content, %
$S_{\text{t,d}}$	true relative density, $\text{g}/\text{cm}^3$
$Q_{\text{b,d}}$	calorific value, MJ/kg
$G_{\text{R,I}}$	clean coal bond index, dimensionless
$C_{\text{daf}}$	fixed carbon content, %
$H_{\text{daf}}$	dry ash-free basis hydrogen content, %
$O_{\text{daf}}$	dry ash-free basis oxygen content, %
$N_{\text{daf}}$	dry ash-free basis nitrogen content, %
$f$	coal hardness coefficient, dimensionless
$\Delta P$	initial velocity of diffusion of coal gas, mmHg
$D_{\text{cf}}$	degree of coal fracturing, dimensionless
$P$	measured coal seam gas pressure, MPa
$TRD$	true relative density of the coal sample, $\text{g}/\text{cm}^3$
$ARD$	apparent relative density of the coal sample, $\text{g}/\text{cm}^3$
$n$	ratio of the total volume of tiny voids to the total volume of coal, %
$a_{\text{ac}}$	maximum gas adsorption capacity, $\text{cm}^3/\text{g}$
$b_{\text{ac}}$	adsorption constant, $\text{MPa}^{-1}$
$Q$	adsorption gas quantity, mL/g

## References

1. Zhao, H.; Lai, Z.; Firoozabadi, A. Sorption Hysteresis of Light Hydrocarbons and Carbon Dioxide in Shale and Kerogen. *Sci. Rep.* **2017**, *7*, 16209. [[CrossRef](#)] [[PubMed](#)]
2. Dejam, M.; Hassanzadeh, H.; Chen, Z. Semi-analytical solutions for a partially penetrated well with wellbore storage and kkin effects in a double-porosity system with a gas cap. *Transp. Porous Media* **2013**, *100*, 159–192. [[CrossRef](#)]
3. Zou, Y.H.; Zhang, Q.H. Technical progress of direct determination of coal seam gas content in coal mines in China. *Min. Saf. Environ. Prot.* **2009**, *36*, 180–183. [[CrossRef](#)]

4. Jiang, W.Z.; Qin, Y.J.; Zou, Y.H.; Dong, J.; Xue, J.F.; Wu, Q.; Zhang, Q.H.; Zhang, S.T. *The Direct Method of Determining Coalbed Gas Content in the Mine*; The General Administration of Quality Supervision, Inspection and Quarantine of the People's Republic of China & the National Standardization Administration of China: Beijing, China, 2009; pp. 3–11.
5. Jin, Z.; Firoozabadi, A. Phase behavior and flow in shale nanopores from molecular simulations. *Fluid Phase Equilib.* **2016**, *430*, 156–168. [[CrossRef](#)]
6. Bertard, C.; Bruyet, B.; Gunther, J. Determination of desorbable gas concentration of coal direct method. *Rock Mech. Min. Sci.* **1970**, 43–65. [[CrossRef](#)]
7. Mcculloch, C.M.; Levine, J.R.; Kissell, F.N.; Deul, M. *Measuring the Methane Content of Bituminous Coalbed*; Department of the Interior Bureau of Mines Ri: Pittsburgh, PA, USA, 1975; p. 8043.
8. Ulery, J.P.; Hyman, D.M. The Modified Direct Method of Gas Content Determination: Application and Results. In Proceedings of the Coalbed Methane Symposia, The University of Alabama, Tuscaloosa, AL, USA, 17–21 May 1991; pp. 489–500.
9. Mavor, M.J.; Pratt, T.J. *Improved Methodology for Determining Total Gas Content, Vol. II. Comparative Evaluation of the Accuracy of Gas-in-Place Estimates and Review of Lost Gas Models*; Gas Research Inst., Topical Rep: Chicago, IL, USA, 1996.
10. Abate, A.F.; Nappi, A.; Narducci, F.; Ricciardi, S. A mixed reality system for industrial environment: An evaluation study. *CAAI Trans. Intell. Technol.* **2017**, *2*, 227–245.
11. Saghafi, A.; Williams, D.J.; Roberts, D.B. *Determination of Coal Gas Content by Quick Crushing Method*; CSIRO Investigation Report: Canberra, Australia, 1995.
12. Smith, D.M.; Williams, F.L. A new technique for determining the methane content of coal. In Proceedings of the 16th Intersociety Energy Conversion Engineering Conference, New York, NY, USA, 9–14 August 1981; pp. 1272–1277.
13. Chase, R.W. *A Comparison of Methods Used for Determining the Natural Gas Content of Coalbeds from Exploratory Cores*; US Department of Energy: Washington, DC, USA, 1979.
14. Sawyer, W.K.; Zuber, M.D.; Kuuskraa, V.A.; Homer, D.M. Using reservoir simulation and field data to define mechanisms controlling coalbed methane production. In Proceedings of the Coalbed Methane Symposia, The University of Alabama, Tuscaloosa, AL, USA, 16–19 November 1987; pp. 295–307.
15. Chen, Y.; Yang, D.; Tang, J.; Li, X.; Jiang, C. Determination method of initial gas desorption law of coal based on flow characteristics of convergent nozzle. *J. Loss Prev. Process Ind.* **2018**, *54*, 222–228. [[CrossRef](#)]
16. Chen, J.W.; Zhang, R.L.; Chai, L. Analysis of sampling loss in the measurement of original gas content in coal seam with downhole desorption method. *Saf. Coal Mines* **2010**, *41*, 84–86. [[CrossRef](#)]
17. Lei, X.R.; Li, H.L.; Hou, H.H. Discussion on the calculation of desulfuration in detecting gas content in coal seam by desorption method. *Coal Mine Mod.* **2012**, *1*, 57–59. [[CrossRef](#)]
18. Zhang, X.Y.; Guo, M.Z.; Song, C.Y.; Gao, L.Q. Comparison and Analysis of Three Methods for Calculating Gas Loss in Coal Seam Gas Content Determination by Desorption Method. *Saf. Coal Mines* **2012**, *43*, 177–185. [[CrossRef](#)]
19. Li, Y.C.; Yang, S.Q. Comparative Analysis of Calculation Methods of Gas Loss. *Saf. Coal Mines* **2012**, *43*, 166–168. [[CrossRef](#)]
20. Wang, J.; Kong, B.; Mei, T.; Wei, H. A lane detection algorithm based on temporal–spatial information matching and fusion. *CAAI Trans. Intell. Technol.* **2017**, *2*, 275–291.
21. Scott, A.R. Hydrogeologic factors affecting gas content distribution in coal beds. *Int. J. Coal Geol.* **2002**, *50*, 363–387. [[CrossRef](#)]
22. Li, X.L.; Wang, E.Y.; Li, Z.H.; Liu, Z.T.; Song, D.Z.; Qiu, L.M. Rock burst monitoring by integrated microseismic and electromagnetic radiation methods. *Rock Mech. Rock Eng.* **2016**, *49*, 4393–4406. [[CrossRef](#)]
23. Liu, Y.; Wang, D.; Hao, F.; Liu, M.J.; Mitri, H.S. Constitutive model for methane desorption and diffusion based on pore structure differences between soft and hard coal. *Int. J. Min. Sci. Technol.* **2017**, *27*, 937–944. [[CrossRef](#)]
24. Cao, J.; Sun, H.T.; Dai, L.C.; Sun, D.L.; Wang, B.; Miao, F.T. Simulation research on dynamic effect of coal and gas outburst. *J. China Univ. Min. Technol.* **2018**, *47*, 113–120. [[CrossRef](#)]
25. Li, Z.Q.; Cheng, Q.; Liu, Y.W.; Duan, Z.P.; Song, D.Y. Research on gas diffusion model and experimental diffusion characteristic of cylindrical coal. *J. China Univ. Min. Technol.* **2017**, *46*, 1033–1040. [[CrossRef](#)]
26. Tang, J.; Jiang, C.; Chen, Y.; Li, X.; Wang, G.; Yang, D. Line prediction technology for forecasting coal and gas outbursts during coal roadway tunneling. *J. Nat. Gas Sci. Eng.* **2016**, *34*, 412–418. [[CrossRef](#)]

27. Yan, G.Q.; Wang, G.; Xin, L.; Du, W.Z.; Huang, Q.M. Direct fitting measurement of gas content in coalbed and selection of reasonable sampling time. *Int. J. Min. Sci. Technol.* **2017**, *27*, 299–305. [[CrossRef](#)]
28. Barrer, R.M. Gas flow in solids. *Philos. Mag.* **1939**, *28*, 148–162. [[CrossRef](#)]
29. Winter, K.; Janas, H. Gas emission characteristics of coal and methods of determining the desorbable gas content by means of desorbometers. In Proceedings of the 16th International Conference on Coal Mine Safety Research, Washington, DC, USA, 22–26 September 1996.
30. Wang, Y.A.; Yang, S.J. Some characteristic of coal seams with hazard of outburst. *J. Chin. Chem. Soc.* **1980**, *1*, 47–53. [[CrossRef](#)]
31. Kang, J.N. Application of direct determination technology of coal seam content in gas drainage effect evaluation of Zhongliang coal mine. *Min. Saf. Environ. Prot.* **2010**, *37*, 31–33. [[CrossRef](#)]
32. Yu, Q.X. *Coal Mine Gas Control*; China University of Mining and Technology Press: Xuzhou, China, 2012; pp. 34–37. ISBN 978-7-5646-1607-6.
33. Zou, Q.L.; Lin, B.Q.; Liu, T.; Zhou, Y.; Zhang, Z.; Yan, F.Z. Variation of methane adsorption property of coal after the treatment of hydraulic slotting and methane pre-drainage: A case study. *J. Nat. Gas Sci. Eng.* **2014**, *20*, 396–406. [[CrossRef](#)]
34. Sun, G.; Li, Y.H.; Wu, K.H.; Gong, X.L.; Tian, X.H.; Pan, M.G. *Sampling of Coal Seams*; The General Administration of Quality Supervision, Inspection and Quarantine of the People’s Republic of China & the National Standardization Administration of China: Beijing, China, 2008; pp. 1–4.
35. Qi, Q.X.; Li, J.Q.; Mao, D.B.; Fu, J.X.; Zhang, X.L. *Methods for Determining Coal Hardness Coefficient*; The General Administration of Quality Supervision, Inspection and Quarantine of the People’s Republic of China & the National Standardization Administration of China: Beijing, China, 2010; pp. 2–3.
36. Han, L.T.; Lin, Y.J.; Chen, K.Q. *Proximate Analysis of Coal*; The General Administration of Quality Supervision, Inspection and Quarantine of the People’s Republic of China & the National Standardization Administration of China: Beijing, China, 2008; pp. 1–9.
37. Qi, Q.X.; Li, J.Q.; Mao, D.B.; Fu, J.X.; Zhang, X.L. *Methods for Determining the Block Density of Coal and Rock*; The General Administration of Quality Supervision, Inspection and Quarantine of the People’s Republic of China & the National Standardization Administration of China: Beijing, China, 2009; pp. 1–6.
38. Zhang, Q.L.; Zhang, S.A. *Experimental Method of High-Pressure Adsorption Isothermal to Coal—Capacity Method*; The General Administration of Quality Supervision, Inspection and Quarantine of the People’s Republic of China & the National Standardization Administration of China: Beijing, China, 2008; pp. 1–5.
39. Hu, Q.T.; Zhao, X.S.; Zou, Y.H.; Li, Q.L.; Kang, J.N.; Zhang, Q.H.; Lei, H.Y. *Specification for Identification of Coal and Gas Outburst Mine*; State Administration of Work Safety: Beijing, China, 2006; pp. 1–6.
40. Li, X.L.; Li, Z.H.; Wang, E.Y.; Liang, Y.P.; Li, B.L.; Chen, P.; Liu, Y.J. Pattern recognition of mine microseismic (MS) and blasting events based on wave fractal features. *Fractals* **2018**, *26*, 1850029. [[CrossRef](#)]

